ACS chemical biology

Articles

pubs.acs.org/acschemicalbiology

Inhibition of the Flavin-Dependent Monooxygenase Siderophore A (SidA) Blocks Siderophore Biosynthesis and *Aspergillus fumigatus* Growth

Julia S. Martín del Campo,[†] Nancy Vogelaar,[‡] Karishma Tolani,[†] Karina Kizjakina,[†] Kim Harich,[†] and Pablo Sobrado*[,†,‡]

[†]Department of Biochemistry, Virginia Tech, Blacksburg, Virginia 24061, United States

[‡]Virginia Tech Center for Drug Discovery, Virginia Tech, Blacksburg, Virginia 24061, United States

Supporting Information

ABSTRACT: *Aspergillus fumigatus* is an opportunistic fungal pathogen and the most common causative agent of fatal invasive mycoses. The flavin-dependent monooxygenase siderophore A (SidA) catalyzes the oxygen and NADPH dependent hydroxylation of L-ornithine (L-Orn) to N^5-L-hydroxyornithine in the biosynthetic pathway of hydroxamate-containing siderophores in *A. fumigatus*. Deletion of the gene that codes for SidA has shown that it is essential in establishing infection in mice models. Here, a fluorescence polarization high-throughput assay was used to screen a 2320 compound library for inhibitors of SidA. Celastrol, a natural quinone methide, was identified as a noncompetitive inhibitor of SidA with a MIC value of 2 μM. Docking experiments suggest that celastrol binds across the NADPH and L-Orn pocket. Celastrol prevents *A. fumigatus* growth in blood agar. The addition of purified ferric-siderophore abolished the inhibitory effect of celastrol. Thus, celastrol inhibits *A. fumigatus* growth by blocking siderophore biosynthesis through SidA inhibiton.

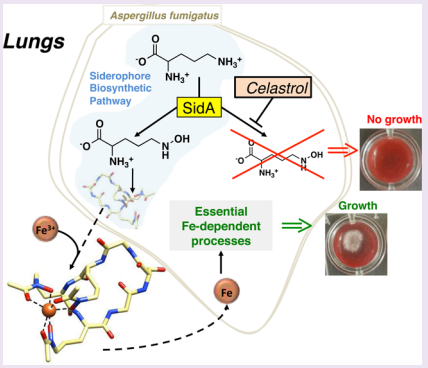

Aspergillus fumigatus is a ubiquitous, saprophytic fungus. In immunocompromised individuals, it often causes infections known as invasive aspergillosis. In susceptible individuals, *A. fumigatus* can cause allergic bronchopulmonary aspergillosis (ABA), and it has been estimated that more than 5 million people worldwide suffer from ABA.[1] Although there are treatments for *A. fumigatus* infections, the mortality rate among immunocompromised patients is >50%, and drug resistance has been reported.[2,3] Thus, new and effective treatments for *A. fumigatus* infections are needed.[4] *A. fumigatus* can survive and grow under a wide range of environmental conditions, including those with limited essential nutrients, such as iron.[5,6] Although abundant on the earth's crust, the bioavailability of iron is low due to its reaction with oxygen, which leads to the formation of insoluble ferric hydroxides. In humans, the availability of free iron is even more limited because it is found in complex with iron-binding molecules, e.g., hemoglobin and myoglobin. These molecules are responsible for lowering the free iron concentration in human serum to 10^{-24} M.[7] During infection, the level of free iron is further decreased by the increased levels of ferritin and the release of lactoferrin from neutrophils.[8] This mechanism of defense has been termed "nutritional immunity."[7] To overcome the iron starvation conditions present in humans, *A. fumigatus* turns on its siderophore-assisted iron uptake machinery.[9] *A. fumigatus* produces four hydroxamate containing siderophores: ferricrocin (FC) and hydroxyferricrocin (HFC) for intracellular iron trafficking and fusarinine C (FsC) and its derivative triacetylfusarinine C (TAFC) for extracellular iron scavenging.[10−12] The first step in the biosynthesis of all four hydroxamate-containing siderophores is catalyzed by the enzyme siderophore A (SidA).[12,13] Deletion of the gene coding for SidA (Δ*sidA*) results in a strain unable to produce siderophores. Siderophores are essential for pathogenesis as the Δ*sidA A. fumigatus* strain is unable to establish infection in a mouse model of invasive aspergillosis.[9,14] These findings identify SidA as an attractive drug target for the treatment of *A. fumigatus* infections.

SidA is an *N*-hydroxylating flavin-containing monooxygenase that catalyzes the NADPH- and oxygen-dependent *N*-hydroxylation of L-ornithine (L-Orn) to produce N^5-hydroxy-L-Ornithine (HO-Orn), which is subsequently incorporated into siderophores to make the iron binding hydroxamate moiety (Figure 1). The crystal structure and detailed biochemical characterization of SidA have been reported.[15−19] Binding of NADPH and reduction of the FAD initiate the reaction. $NADP^+$ remains bound and plays a role in stabilization of the C4a-hydroperoxyflavin (FAD_{OOH}) intermediate, which is essential for hydroxylation.[16,17] The structure of the SidA-$NADP^+$ complex shows that $NADP^+$ binds in an

Received: August 3, 2016
Accepted: September 2, 2016
Published: September 2, 2016

DOI: 10.1021/acschembio.6b00666
ACS Chem. Biol. 2016, 11, 3035−3042

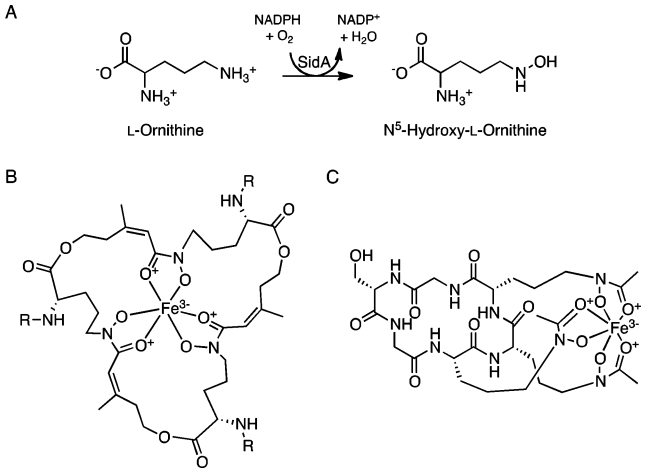

Figure 1. (a) Reaction catalyzed by the enzyme SidA. (b and c) Ferric complexes of the siderophores produced by *A. fumigatus*. In b, when R = H, the siderophores is fusarinine C (FsC), and when R = acetyl, the siderophores is TAFC. In c, ferricrocin is shown.

extended conformation, with the nicotinamide moiety binding close to the FAD and the adenosine diphosphate (ADP) binding away from the active site.[15] Previously, we developed a fluorescence polarization (FP) binding assay for SidA by covalently linking a TAMRA chromophore to ADP. The ADP-TAMRA was shown to be a good probe for the identification of small molecules that bound to the active site of SidA using FP.[20]

In this work, we optimized the ADP-TAMRA FP assay conditions in order to perform high-throughput screening (HTS) of a 2320 compound library to identify inhibitors of SidA. We also implemented an orthogonal secondary assay based on enzyme activity to eliminate false positives. This approach allowed us to identify celastrol as a specific SidA inhibitor. We showed that celastrol inhibits siderophore biosynthesis in *A. fumigatus* and, as a consequence, cellular growth. This report provides an effective procedure for the identification of inhibitors of siderophore biosynthesis in fungi, validates SidA as a drug target, and identifies celastrol as a potential drug against *A. fumigatus* and other fungi.

RESULTS

High-Throughput Screening Assay. The Spectrum Collection library (2320 compounds) was screened against SidA at 20 μM concentration (2% DMSO) using ADP-TAMRA as described in the Methods section.[20] We selected the Spectrum library because it is composed of bioactive compounds (60%), natural compounds of unknown biological properties (25%), and compounds representative of known-drug enzyme inhibitors, among others. The Z′ factor was calculated to be 0.74 ± 0.04, which indicates a wide separation between positive and negative controls. The process of positive hit validation and inhibitor selection is described in Figure 2. Positive hits were defined as those compounds that reduced the anisotropy below 66%. Following this criterion, 32 compounds were identified as positive hits in the FP assay (Table S1). The ability of these compounds to inhibit SidA activity was tested using a colorimetric activity assay. Only 37% (12 compounds) were shown to decrease activity in the colorimetric assay. It was found that 33% of these compounds were false positives, as they prevented color development, leaving only eight compounds for further analysis. The possibility that the observed enzyme inhibition was originated by NADPH depletion was assessed using a hydrogen peroxide production assay to test the oxidation of NADPH by the compounds. Removing the compounds that reacted with NADPH reduced the selection to celastrol, dihydrocelastrol, and 4,4′-diisothiocyano-2,2′-stilbenedisulfonic acid (DIDS). DIDS has been shown to be an anion transport inhibitor that binds covalently to the outer surface of the human erythrocyte membrane protein and inhibits ATP-translocation through the endoplasmic reticulum membrane of yeast and mammalian microsomes.[21,22] DIDS had a relatively low binding affinity to SidA (IC_{50}= 103 ± 5 μM); therefore, was not studied further.

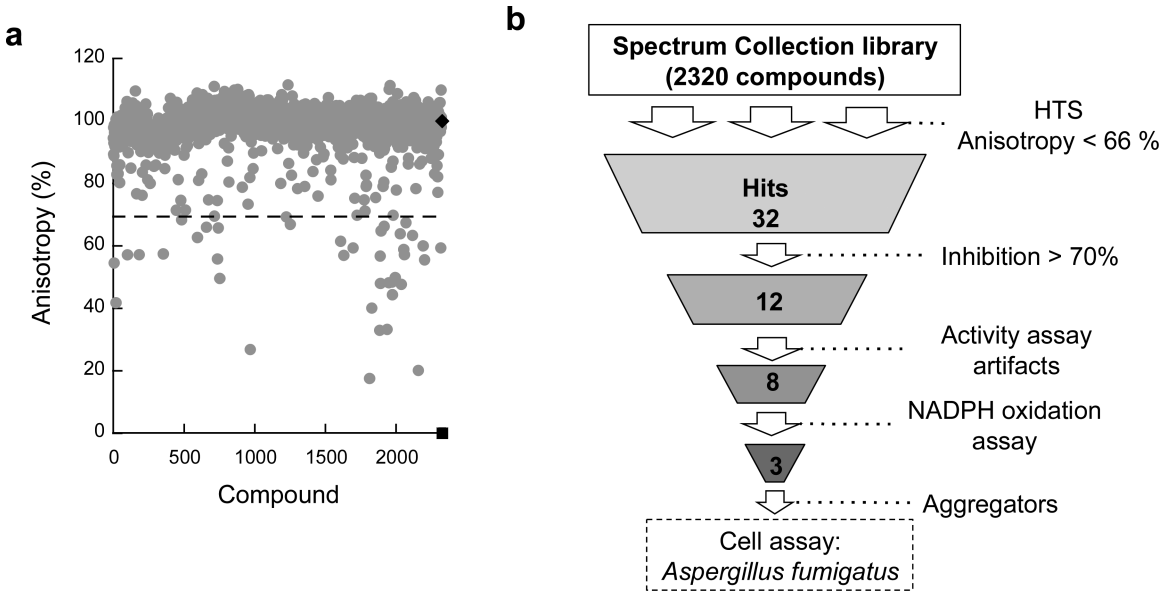

Figure 2. (a) HTS of spectrum library against SidA. Negative control (♦) consists of SidA and ADP-TAMRA, and positive control (■) corresponds to ADP-TAMRA. (b) Summary of procedures used to validate positive hits.

DOI: 10.1021/acschembio.6b00666
ACS Chem. Biol. 2016, 11, 3035−3042

Mechanism of Inhibition. The IC_{50} of celastrol and dihydrocelastrol in 10% DMSO was determined with a 10-point dose−response curve using the colorimetric activity assay and verified with the UPLC product detection assay (Figure 3 and Table 1). Inhibition by aggregation was assessed with the activity assay using a 10-point dose−response curve in the presence of 0.1% triton X-100 and 10% DMSO. No change in IC_{50} value was observed for celastrol, while a positive shift for the IC_{50} curve for dihydrocelastrol was observed (IC_{50} ~ 1 mM, not shown), indicating that SidA inhibition by dihydrocelastrol occurs via aggregation.[23] We further verified that celastrol is not a SidA denaturant by measuring the melting temperature (T_m) at different celastrol concentrations using the ThermoFAD assay and 2% DMSO.[24] The T_m in the absence of ligand was ~48 °C, and upon binding either $NADP^+$ or L-Orn, no major changes in the T_m value were observed. Similarly, in the presence of celastrol (20 or 110 μM), the calculated T_m values were close to 48 °C (Figure S1 and Table S2).

Protein unfolding studies at celastrol concentrations above 110 μM were not conducted due to the low solubility of the compound in 2% DMSO. These results indicate that the mechanism of celastrol inhibition does not involve destabilization/denaturation of SidA.

The type of inhibition by celastrol was determined by measuring the activity of SidA as a function of L-Orn, NADPH, and celastrol concentrations at 10% DMSO. The results are shown as Lineweaver−Burk plots in Figure 4. The different slopes and *y*-intercept values are consistent with celastrol functioning as a noncompetitive inhibitor for NADPH and L-Orn.

It has been reported that the quinone methide moiety of celastrol can form Michael adducts with nucleophilic residues.[25−27] Because SidA contains five cysteine residues, we tested the possibility that celastrol inhibition occurred *via*

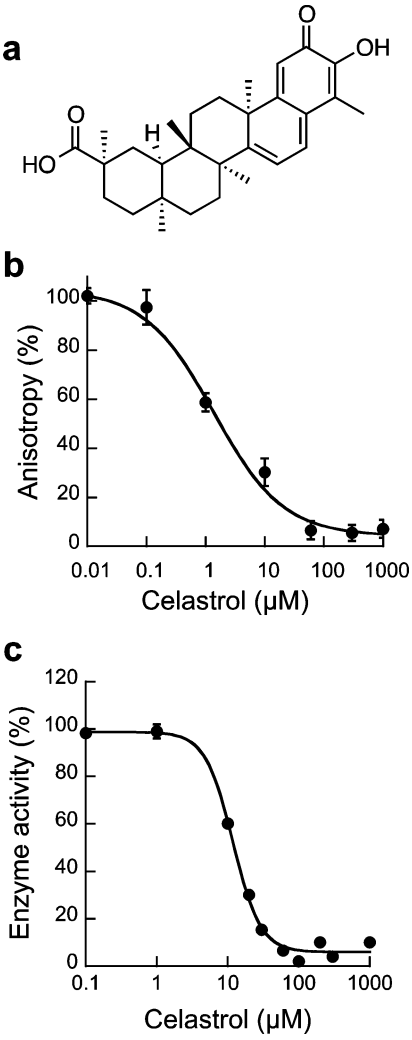

Figure 3. (a) Structure of celastrol, the identified SidA inhibitor with ADP-TAMRA. (b) Binding curve of celastrol to SidA. Dissociation constant was determined using the FP assay. (c) Dose response curve of celastrol inhibition by monitoring L-Orn hydroxylation.

Table 1. IC_{50}, K_D, and K_I Values Determined for Celastrol Binding to SidA[a]

parameter	value (μM)
IC_{50}	11 ± 1
K_D	1.4 ± 0.3
$K_{I(NADPH)}$	4.6 ± 0.3
$K_{I(L\text{-}Orn)}$	6.2 ± 0.7

[a]IC_{50} was obtained with the activity assay and verified with the UPLC. K_D for celastrol was determined using the ADP-TAMRA binding assay.[20] K_I vales (0−13 μM celastrol) were determined with a global fit for non-competitive inhibition using the software GraFit (Erithacus Software Limited, 2012).

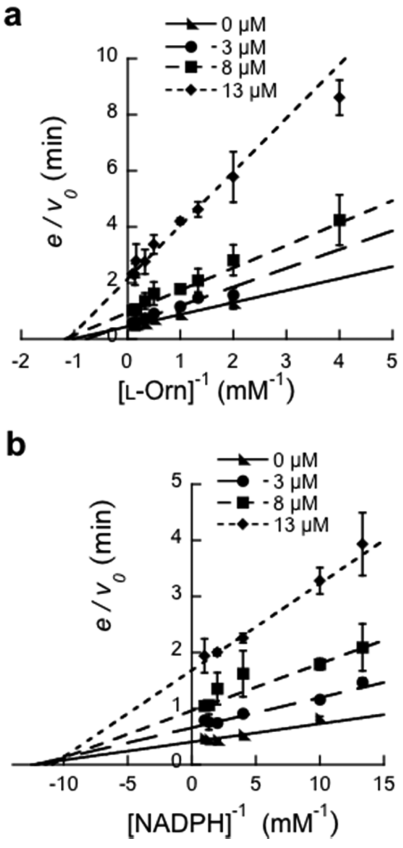

Figure 4. Double-reciprocal plot of varying celastrol concentrations in the presence of varying concentrations of (a) L-Orn (NADPH kept constant at 1 mM) and (b) NADPH (L-Orn kept constant at 10 mM). The K_M values for L-Orn and NADPH are 1 mM and 100 μM, respectively.

DOI: 10.1021/acschembio.6b00666
ACS Chem. Biol. 2016, 11, 3035−3042

the formation of covalent adducts with SidA by incubating the enzyme (10 μM) with a 15-fold excess of celastrol (150 μM) for 30 min at RT followed by dialysis. The activity was unaffected by celastrol after dialysis compared to the DMSO control, indicating the absence of stable covalent adducts between SidA and celastrol. Docking experiments suggest that celastrol might occupy the NADPH binding site (Figure 5). The proposed binding mode shows hydrogen bonds between celastrol and four residues (Ser-254, Gly-255, Ser-257, and Gln-104) and π stacks with the isoalloxazine moiety of FAD.

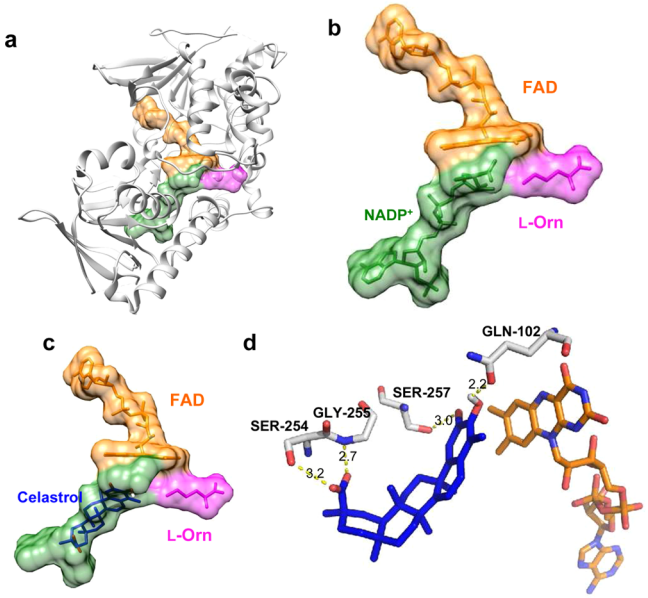

Figure 5. Docking of celastrol in the active site of SidA. (a) FAD, $NADP^+$, and L-Orn surface highlighted in SidA (4B63). (b) Alignment of coenzymes and substrate in binding pocket surface, protein was removed for better visualization. (c) Best predicted celastrol docking pose, obtained when the molecule was docked in 4B63 structure with FAD. (d) Polar contacts are shown in yellow and distances in Å.

Inhibition of *A. fumigatus* Growth by Celastrol. *A. fumigatus* was grown in rich media (PDA) and in defined minimum media without supplemented iron (AMM-Fe) in the presence of celastrol to determine the *in cellulo* effect. Celastrol did not cause growth inhibition in PDA agar, suggesting that it was not toxic at the concentration tested (50 μM). If celastrol is in fact targeting SidA, the growth of *A. fumigatus* in the presence of the inhibitor should resemble the observed phenotype reported for the Δ*sidA A. fumigatus* strain.[9,14] It was reported that the Δ*sidA* strain was unable to grow in blood agar. Our results show that celastrol (50 μM) drastically decreased the growth of *A. fumigatus* in AMM-Fe compared to the DMSO control (Figure 6). In blood agar, after 28 h of incubation at 37 °C, celastrol (50 μM) completely inhibited the growth of *A. fumigatus* compared to the DMSO control. The minimal inhibitory concentration (MIC) was determined to be 2 μM in AMM-Fe (Figure S2).

Growth Rescue by Fe-Siderophores. To verify that the absence of growth was caused by the lack of siderophores due to SidA inhibition, Fe-siderophores (27% FsC, 12% FC, and 61% TAFC) were added to AMM-Fe or blood agar media at concentrations of 0.1 and 10 μM (Figure 6). The composition of siderophore extract was analyzed by HPLC (Figure S3) and the identity of the peaks was confirmed by LC-MS. The observed monoisotopic masses are summarized in Table S3.

The addition of 10 μM siderophores recovered the growth of *A. fumigatus* in AMM-Fe at the level of the DMSO control, while 0.1 μM was insufficient to overcome the SidA inhibition phenotype. The same effect was observed in blood agar. Recovery of growth confirms that the mode of action of celastrol leads to inhibition of the siderophore biosynthetic pathway. To further validate that celastrol was in fact inhibiting siderophore biosynthesis, the effect of celastrol on siderophore production was determined. In this experiment, *A. fumigatus* was grown in drops of AMM-Fe, and mycelia were washed until siderophores were undetectable using Chrome Azurol S.[28] At this point, immobilized mycelia were transferred to fresh AMM-Fe containing either 100 μM celastrol or DMSO. After 3 h of incubation at 37 °C, siderophore quantification in the liquid phase was 140 μM in the DMSO control and near zero

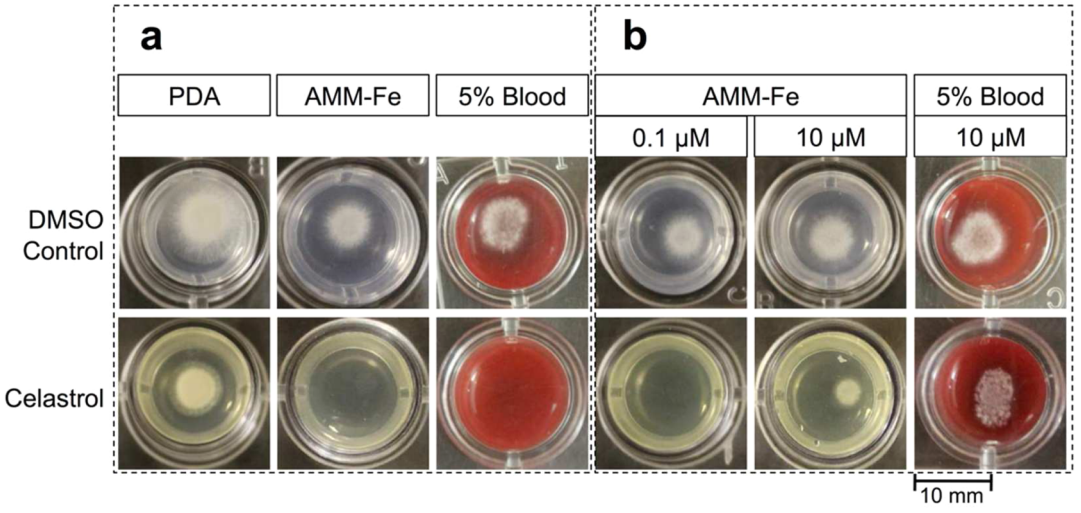

Figure 6. Effect of celastrol in the growth of *A. fumigatus*. Pictures correspond to 28 h of incubation at 37 °C; outside limits of the wells are shown for reference. (a) *A. fumigatus* growth in different media with and without supplemented celastrol. (b) *A. fumigatus* growth in iron limited media with 50 μM celastrol and 0.1 or 10 μM Fe(III)-siderophore.

DOI: 10.1021/acschembio.6b00666
ACS Chem. Biol. 2016, 11, 3035−3042

in the celastrol-treated culture (Figure S4). These findings indicate that inhibition of SidA by celastrol abolishes siderophore biosynthesis and leads to growth inhibition under iron limiting conditions.

DISCUSSION

Iron is essential for the growth and survival of bacteria and fungi, but the concentration of free iron is tightly regulated in the mammalian host. This process is referred to as nutritional immunity, where the expression of a number of iron binding proteins is increased, further decreasing the iron concentration to values not suitable for the rapid microbial growth that is required during infection.[7] However, several bacterial and fungal pathogens circumvent the low iron availability by scavenging iron from the host *via* reductive iron intake and secretion of siderophores.[9,29] It has been shown that siderophore biosynthesis is essential for infection in bacteria and fungi.[9,30,31] Several recent reports have shown that targeting iron acquisition in human pathogens is a viable approach to combat deadly diseases with increasing antibiotic resistance.[32] For example, the marine microbial natural products Baulamycins A and B have been identified as inhibitors of the nonribosomal peptide synthetases SbnE and AsbA involved in the siderophore biosynthesis staphyloferrin in *Spahylococcus aureus* and petrobactin in *Bacillus anthracis*, with IC_{50} values of ∼5−200 μM.[33] Identification of inhibitors of isochorismate-pyruvate lyase in the biosynthesis of pyochelin in *Pseudomonas aeruginosa* were reported to have low micromolar IC_{50} values *in vitro* against the enzyme. However, inhibition of bacterial growth was exhibited at concentrations greater than 5 mM.[34] Inhibition of mycobactin and yersiniabactin by targeting salicylation enzymes with salicyl-AMP derivatives was reported to inhibit bacterial growth at nanomolar concentration.[35] It has been reported that the topical application of iron chelators or statins reduces *Aspergillus fumigatus* and *Fusarium oxysporum* growth in a model of fungal infection of the cornea.[30] A two-stage, cell based screening method for the identification of compounds that interfere in the siderophore production in *A. fumigatus* has been reported.[36] Although the assay lacks target selectivity, it provides a basic approach for the cell-based discovery of inhibitors of the fungal siderophore machinery.

To our knowledge, there have been no reports of selective targeted small molecule inhibition of siderophore biosynthesis in pathogenic fungi.

The structural and biochemical characterization of SidA led us to the rational design of an ADP-TAMRA chromophore optimized for high throughput screening of small molecules that might function as inhibitors of SidA. In our HTS, celastrol was identified as a noncompetitive inhibitor of SidA. Celastrol is a natural quinone methide triterpene, widely found in the plant genuses *Celastrus*, *Maytenus*, and *Tripterygium*.[37] Celastrol has been reported to exhibit bioactive properties as an antioxidant,[38] anti-inflamatory,[39,40] and anticancer compound.[37,41] Celastrol is also a leptin sensitizer and a promising agent for the pharmacological treatment of obesity.[42] It has been reported that celastrol has positive effects on Huntington's and Parkinson's diseases.[43,44] The neurodegenerative protection by celastrol has been proposed to be related to the inhibition of human NADPH oxidase (NOX) isoforms.[45] Similarly, the antimalaria activity of celastrol might be linked to inhibition of the NADH dependent enoyl-acyl carrier protein reductase from *Plasmodium falciparum*.[46] Both NOX and enoyl-acyl carrier protein reductase are NAD(P)H binding proteins. These results are consistent with celastrol targeting SidA in *A. fumigatus*, which also binds NAD(P)H. Our docking studies suggest that celastrol may occupy the NADPH binding site (Figure 5), consistent with the noncompetitive inhibition mechanism. Noncompetitive inhibition by active site-binding inhibitors are common for bisubstrate/biproduct enzymes and enzymes that follow a compulsory order of substrate addition or product release.[47]

We show that inhibition of SidA by celastrol blocks siderophore production, which prevents *A. fumigatus* growth under iron-limiting conditions. This effect is consistent with the observed phenotype of the *A. fumigatus* strain that lacks the gene coding for SidA. The antifungal activity of celastrol was previously reported in the phytopathogen fungi *Glomerella cingulata* and *Fusarium oxysporum*.[48] By examining mutant *Fusarium* strains, it was found that extracellular siderophores are essential for fungal growth during infection by *F. oxysporum*.[30] Amino acid alignment of *A. fumigatus* SidA against the SidA of *G. cingulata* and *Fusarium* revealed an enzyme identity of 47 and 53%, respectively (not shown). This suggests that one possible mechanism of action of celastrol in *G. cingulata* and *Fusarium* might be through SidA inhibition/iron starvation as we have demonstrated in *A. fumigatus*.

This work presents a robust screening methodology, identification, and validation of the natural product celastrol as an antifungal agent. The results further validate siderophore biosynthesis as a drug design target. Celastrol has been shown to have positive effects in humans as an antiobesity compound and as an antineuronal against damage from ROS. Thus, further improvements and selectivity of celastrol inhibition of SidA and related *N*-hydroxylating monooxygenases from fungi and bacteria might lead to compounds with improved antifungal and potentially antibacterial activity.

METHODS

Materials. Buffers and bacterial growth media were obtained from Fisher Scientific (Pittsburgh, PA) and Sigma-Aldrich (St. Louis, MO). Turbo BL21 (DE3) chemically competent cells were obtained from Genlantis (San Diego, CA) and pET-15b vector from Novagen. For protein purification, an AKTA prime system (GE Healthcare) was used along with IMAC columns (GE Healthcare). Acquity ultra-performance liquid chromatography (UPLC) and C18 (2.1 × 10 mm) analytical columns were obtained from Waters. NADH and NADPH were obtained from EMD Biosciences (Billerica, MA). The Spectrum Collection was from Microsource (Gaylordsville, CT). This library is composed of 2320 bioactive compounds. For the FP assay, nonbinding surface black 96-well plates were purchased from Greiner Bio-One (Monroe, NC), and the samples were analyzed on a spectramax M5 microplate spectrophotometer (Molecular Devices, Sunnyvale, CA). Differential scanning fluorimetry was performed in an RT-PCR (Applied Biosystems 7300) using 96-well RT-PCR plates (Microamp 4306737) and optical adhesive film (MicroAmp 431197971). Celastrol was purchased from Cayman Chemical (Ann Arbor, MI). *Aspergillus fumigatus* strain 46645 was purchased from the American Type Culture Collection (ATCC), and tissue culture plates were purchased from MP Biomedicals.

Protein Expression and Purification. The gene coding for *A. fumigatus* SidA was subcloned into the pET-15b vector (Novagen) and expressed as an N-terminus 6xHis tag fusion protein.[15] The plasmid was transformed into Turbo BL21 (DE3) *Escherichia coli* cells (Sigma Chemical Co.) and expressed using autoinduction medium.[49] A total of 6 L of media was incubated at 37 °C with shaking at 250 rpm, to an optical density at 600 nm of 4 followed by overnight incubation at 17 °C. This procedure normally yielded ∼75 g of cells. The cell pellet was frozen at −80 °C. For protein purification, the cell paste was resuspended in 250 mL of buffer A (25 mM HEPES, 300 mM NaCl,

DOI: 10.1021/acschembio.6b00666
ACS Chem. Biol. 2016, 11, 3035−3042

20 mM imidazole, pH 7.5) and incubated with 25 mg mL^{-1} of lysozyme, DNase I, and RNase for 45 min at 4 °C with constant stirring. The resulting solution was sonicated for 15 min at 70% amplitude at cycles of 5 s on and 10 s off. During sonication, the solution was incubated on ice. The lysate was centrifuged at 45 000*g* for 45 min. After this time, the supernatant was collected and loaded onto three in-tandem 5 mL HisTrap columns previously equilibrated with buffer A. After loading was completed, the columns were washed with buffer A until the absorbance at 280 nm returned to baseline levels. The columns were then washed with buffer B (25 mM HEPES, 300 mM NaCl, 75 mM imidazole, pH 7.5). SidA was eluted with buffer C (25 mM HEPES, 300 mM NaCl, 300 mM imidazole, pH 7.5). The buffer of the purified protein was exchanged by dialysis into 100 mM sodium phosphate and 50 mM NaCl, at pH 7.5. The enzyme was concentrated to 100 μM, flash frozen in liquid nitrogen, and stored at −80 °C until use.

High Throughput Screening Assay. High-throughput screening of the Spectrum Collection library using the FP assay designed for SidA was performed at the Virginia Tech Center for Drug Discovery Screening Lab.[20] The 96 well plates were used, and the reaction volume was 25 μL using 50 mM sodium phosphate buffer (pH 7.0). For the screening, 30 nM of ADP-TAMRA with 2 μM SidA (based on the Bradford assay) and 20 μM of library compound were used, with the final DMSO concentration at 2%. Fluorescence polarization measurements were performed with excitation at 544 nm and emission at 584 nm, using a wavelength cutoff of 570 nm. Anisotropy values were normalized to the values obtained in the negative control sample: SidA, ADP-TAMRA, and DMSO. The positive control consisted of ADP-TAMRA and DMSO. The Z prime (Z') value was determined using eq 1 where, $\sigma_{N,P}$ and $\mu_{N,P}$ represent the standard deviation and the mean value of the negative and positive controls, respectively.

$$Z' = 1 - \frac{3(\sigma_N + \sigma_P)}{|\mu_N - \mu_P|} \quad (1)$$

Activity Assay, IC_{50}, and K_i Determination. The amount of hydroxylated product was measured using a variation of the Csaky iodine assay. Briefly, this assay consists of the formation of nitrite from hydroxyl amine that is quantified by formation of a chromophore with α-naphthylamine, which has an absorbance maximum at 529 nm.[50,51] Formation of HO-Orn was quantified using a standard curve with hydroxylamine (25−350 μM). The standard assay contained 25 μL of 100 mM sodium phosphate (pH 7.5), 1 μM SidA, 500 μM L-Orn, and 250 μM NADPH for activity and IC_{50} determinations. Compound concentration was varied from 0.01 to 1 mM, and the reaction mix contained a final DMSO concentration of 10%. The reaction was started with the addition of NADPH, allowed to proceed for 20 min at RT, and quenched with 13 μL of 2 N $HClO_4$. To identify compounds that caused inhibition by inducing protein aggregation, the IC_{50} was determined in 100 mM phosphate buffer, pH 7.5, containing 0.1% v/v Triton X-100.[23] As some compounds had either an increase or decrease in the color development or had absorbance at a visible wavelength, 100 μM hydroxylamine was mixed with a series of compound concentrations (0.01 to 1 mM) and treated for color development to identify false positives. The inhibition constant (K_I) was determined by measuring the amount of HO-Orn. When the concentration of L-Orn was varied (0 to 10 mM), NADPH was kept constant at 1 mM, and when the concentration of NADPH was the varied (0 to 1 mM), L-Orn substrate concentration was kept constant at 10 mM. In addition to the colorimetric assay, formation of HO-Orn was quantified following a reported method for HPLC with adaptations for UPLC.[52,53] To determine hydroxylation of L-Orn, SidA (1 μM) was mixed with 250 μM NADPH and 500 μM L-Orn in 100 μL of 50 mM Tris-HCl, pH 8.0, for 20 min. The reaction was quenched with 200 μL of 100% acetonitrile and centrifuged at 13 000 rpm for 1 min to remove protein. A total of 130 μL of supernatant was withdrawn and combined with 25 μL of 200 mM borate, pH 8.0. L-Orn and its hydroxylated product were derivatized by the addition of 3.4 μL of 150 mM FMOC-Cl followed by 5 min incubation at 25 °C. To remove any excess FMOC-Cl, 158 μL of 1-aminoadamantane (53 mM) was added and incubated at RT for an additional 15 min. The samples were analyzed by reverse phase UPLC by loading 1 μL onto a C18 column equilibrated in 60% eluent A (0.1% trifluoroacetic acid in water) with a flow of 0.5 mL/min. The samples were eluted with a linear gradient from 40 to 100% eluent B (0.1% trifluoroacetic acid in acetonitrile) over 10 min and monitored at 263 nm.

Hydrogen Peroxide Quantification Assay. To identify false positive hits that decreased the activity of SidA by oxidation of NADPH, we screened the formation of hydrogen peroxide (H_2O_2) in the absence of SidA using the xylenol orange assay.[54] The assay solution consisted of 30 μL of 50 mM HEPES buffer (pH 7.5) containing 200 mM NaCl, 500 μM NADPH, and 200 μM of compound (dissolved in DSMO). The final DMSO concentration in the reaction mix was 10%. Controls contained DMSO instead of compound. The reaction was started by the addition of NADPH and was allowed to proceed at RT in the dark. After 45 min, the reaction was quenched with 225 μL of a freshly made solution of 200 mM sorbitol, 250 μM xylenol orange, 500 μM ammonium ferrous sulfate, and 25 mM sulfuric acid. After 10 min of incubation, the absorbance was measured at 595 nm. The concentration of H_2O_2 in samples was determined by comparison with a predetermined H_2O_2 standard curve.

ThermoFAD Assay. The melting temperature (T_m) of SidA was determined by measuring the FAD fluorescence as a function of temperature (20−90 °C, 1 °C step) following the reported procedures.[24] The reaction solution consisted of 20 μL of 3 mg mL^{-1} SidA, 2% DMSO in 50 mM potassium phosphate buffer at pH 7.0, and 2% DMSO. As a reference, the T_m was calculated in the presence of L-Orn (100 mM) and $NADP^+$ (12.5 mM). Celastrol was added at 20 and 110 μM.

Docking Studies. The docking studies were conducted in Autodock − Vina[55] using the reported protein structure for SidA with PDB registry 4B63.[15] The structure of celastrol was prepared using Dock Prep.[56] $NADP^+$ and the substrate L-Orn were subtracted from the structure, and the FAD cofactor was retained in the binding pocket. Celastrol was docked in the $NADP^+$-L-Orn cavity using the center coordinates box $x = -20.7175$, $y = -31.4803$, and $z = 9.32009$ and the box size $x = 19.5469$, $y = 24.0362$, and $z = 16.5189$. For the preparation of the receptor, hydrogen atoms were added, charges were merged, and nonpolar hydrogen was removed. FAD was not ignored. For celastrol, the charges were merged, nonpolar hydrogens and lone pairs removed, and charges merged. In all experiments, the predicted free binding energies ranged from −4.1 to −6.5 kcal/mol.

Fe-Siderophore Isolation and Quantification. A 100 mL culture of *A. fumigatus* inoculated with a spore concentration of 1×10^6 was grown in Aspergillus minimum media (AMM) without supplemented iron (AMM-Fe) for 72 h with shaking at 37 °C.[9] The culture was filtered with a 0.2 μm membrane, and $FeCl_3$ was added to the filtrate to a final concentration of 1.5 mM. The resulting brown solution was passed through an Amberlite XAD-2 column. After washing the column with three column volumes of water, Fe(III)-siderophores were eluted with one column volume of methanol.[57] Concentration of total Fe(III)-siderophores was estimated at 435 nm, using the extinction coefficient 2.46 mM^{-1} cm^{-1}.[57] Purified siderophores were filtered through a 0.2 μm membrane before being injected into the HPLC. Separation was performed by reverse-phase HPLC (Phenomenex Luna C18 column, 250 × 4.6 mm, 5 μm). The flow rate of the mobile phase was 1 mL/min, and the injection volume was 50 μL. The binary gradient consisted of 0.1% aqueous formic acid (solvent A) and methanol (solvent B) with a linear gradient from 0 to 100% B over 40 min and monitored at 435 nm. Identity of peaks was confirmed by LC-MS, and the composition of the sample was estimated based on peak area.

Growth Inhibition. Spores of *A. fumigatus* from ATCC were germinated in potato dextrose agar (PDA). Spores were harvested using a sterile plastic scraper from 2 day old cultures grown at 37 °C and suspended in phosphate saline buffer containing 0.1% Tween-20. For inhibition assays, *A. fumigatus* was grown on AMM-Fe and in blood agar (5% sheep blood in AMM-Fe) following the reported procedure.[9] Inhibition of growth was tested in 24-well plates containing 500 μL of agar at a final DMSO concentration of 0.1%.

DOI: 10.1021/acschembio.6b00666
ACS Chem. Biol. 2016, 11, 3035−3042

DMSO and 27 μM amphotericin B were used as negative and positive controls, respectively. DMSO, celastrol, and amphotericin B were well-mixed with agar before jellifying. Wells were point inoculated with 2 μL of 5×10^5 spores/mL and incubated at 37 °C. Minimum inhibitory concentration (MIC) for celastrol was determined in AMM-Fe medium using the standard agar dilution method with a final DMSO concentration of 0.1%. MIC was defined as the minimum concentration of celastrol at which no visible growth was observed after 24 h of incubation at 37 °C.

Growth Rescue. To rescue cell-growth upon SidA inhibition, Fe(III)-siderophore extract was supplemented in the agar-minimum media in the presence of 50 μM celastrol. The estimated concentration of siderophore supplemented in the agar was 0.1 and 10 μM. The extract consisted of 27% FsC, 12% FC, and 61% TAFC. Wells were spot inoculated with 2 μL of 5×10^5 spores/mL and incubated at 37 °C.

■ ASSOCIATED CONTENT

Supporting Information

The Supporting Information is available free of charge on the ACS Publications website at DOI: 10.1021/acschembio.6b00666.

Tables S1 to S3 and Figures S1 to S4 (PDF)

■ AUTHOR INFORMATION

Corresponding Author

*E-mail: psobrado@vt.edu.

Author Contributions

All authors have given approval to the final version of the manuscript.

Funding

This work was funded in part by NSF-MCB-1021384.

Notes

The authors declare no competing financial interest.

■ REFERENCES

(1) Agarwal, R., Chakrabarti, A., Shah, A., Gupta, D., Meis, J. F., Guleria, R., Moss, R., and Denning, D. W. (2013) Allergic bronchopulmonary aspergillosis: review of literature and proposal of new diagnostic and classification criteria. *Clin. Exp. Allergy 43*, 850−873.

(2) Snelders, E., van der Lee, H. A. L., Kuijpers, J., Rijs, A. J. M. M., Varga, J., Samson, R. A., Mellado, E., Donders, A. R. T., Melchers, W. J. G., and Verweij, P. E. (2008) Emergence of Azole Resistance in Aspergillus fumigatus and Spread of a Single Resistance Mechanism. *PLoS Med. 5*, e219.

(3) Brown, G. D., Denning, D. W., Gow, N. A. R., Levitz, S. M., Netea, M. G., and White, T. C. (2012) Hidden Killers: Human Fungal Infections. *Sci. Transl. Med. 4*, 165rv113−165rv113.

(4) Schlamm, H. T., and Marr, K. A. (2015) Combination Therapy for Invasive Aspergillosis: Controversies and Conclusions. *Curr. Fungal Infect. Rep. 9*, 130−134.

(5) Kwon-Chung, K. J., and Sugui, J. A. (2013) Aspergillus fumigatus What Makes the Species a Ubiquitous Human Fungal Pathogen? *PLoS Pathog. 9*, e1003743.

(6) Schrettl, M., and Haas, H. (2011) Iron homeostasis, Achilles' heel of Aspergillus fumigatus? *Curr. Opin. Microbiol. 14*, 400−405.

(7) Potrykus, J., Ballou, E. R., Childers, D. S., and Brown, A. J. P. (2014) onflicting Interests in the Pathogen−Host Tug of War: Fungal Micronutrient Scavenging Versus Mammalian Nutritional Immunity. *PLoS Pathog. 10*, e1003910.

(8) Hissen, A. H. T., Chow, J. M. T., Pinto, L. J., and Moore, M. M. (2004) Survival of Aspergillus fumigatus in Serum Involves Removal of Iron from Transferrin: the Role of Siderophores. *Infect. Immun. 72*, 1402−1408.

(9) Schrettl, M., Bignell, E., Kragl, C., Joechl, C., Rogers, T., Arst, H. N., Haynes, K., and Haas, H. (2004) Siderophore biosynthesis but not Reductive Iron Assimilation is essential for *Aspergillus fumigatus* virulence. *J. Exp. Med. 200*, 1213−1219.

(10) Haas, H. (2014) Fungal siderophore metabolism with a focus on Aspergillus fumigatus. *Nat. Prod. Rep. 31*, 1266−1276.

(11) Schrettl, M., Bignell, E., Kragl, C., Sabiha, Y., Loss, O., Eisendle, M., Wallner, A., Arst, H. N., Jr., Haynes, K., and Haas, H. (2007) Distinct Roles for Intra- and Extracellular Siderophores during Aspergillus fumigatus Infection. *PLoS Pathog. 3*, e128.

(12) Blatzer, M., Schrettl, M., Sarg, B., Lindner, H. H., Pfaller, K., and Haas, H. (2011) SidL, an Aspergillus fumigatus Transacetylase Involved in Biosynthesis of the Siderophores Ferricrocin and Hydroxyferricrocin. *Appl. Environ. Microbiol. 77*, 4959−4966.

(13) Haas, H. (2012) Iron - a key nexus in the virulence of Aspergillus fumigatus. *Front. Microbiol. 3*, 28.

(14) Hissen, A. H. T., Wan, A. N. C., Warwas, M. L., Pinto, L. J., and Moore, M. M. (2005) The Aspergillus fumigatus Siderophore Biosynthetic Gene sidA, Encoding L-Ornithine N5-Oxygenase, Is Required for Virulence. *Infect. Immun. 73*, 5493−5503.

(15) Franceschini, S., Fedkenheuer, M., Vogelaar, N. J., Robinson, H. H., Sobrado, P., and Mattevi, A. (2012) Structural Insight into the Mechanism of Oxygen Activation and Substrate Selectivity of Flavin-Dependent N-Hydroxylating Monooxygenases. *Biochemistry 51*, 7043−7045.

(16) Robinson, R., Badieyan, S., and Sobrado, P. (2013) C4a-Hydroperoxyflavin Formation in N-Hydroxylating Flavin Monooxygenases Is Mediated by the 2′-OH of the Nicotinamide Ribose of NADP+. *Biochemistry 52*, 9089−9091.

(17) Chocklett, S. W., and Sobrado, P. (2010) Aspergillus fumigatus SidA Is a Highly Specific Ornithine Hydroxylase with Bound Flavin Cofactor. *Biochemistry 49*, 6777−6783.

(18) Shirey, C., Badieyan, S., and Sobrado, P. (2013) Role of Ser-257 in the Sliding Mechanism of NADP(H) in the Reaction Catalyzed by the Aspergillus fumigatus Flavin-dependent Ornithine N5-Monooxygenase SidA. *J. Biol. Chem. 288*, 32440−32448.

(19) Robinson, R., Franceschini, S., Fedkenheuer, M., Rodriguez, P. J., Ellerbrock, J., Romero, E., Echandi, M. P., Martin del Campo, J. S., and Sobrado, P. (2014) Arg279 is the key regulator of coenzyme selectivity in the flavin-dependent ornithine monooxygenase SidA. *Biochim. Biophys. Acta, Proteins Proteomics 1844*, 778−784.

(20) Qi, J., Kizjakina, K., Robinson, R., Tolani, K., and Sobrado, P. (2012) A fluorescence polarization binding assay to identify inhibitors of flavin-dependent monooxygenases. *Anal. Biochem. 425*, 80−87.

(21) Gasbjerg, P., Funder, J., and Brahm, J. (1993) Kinetics of residual chloride transport in human red blood cells after maximum covalent 4,4′-diisothiocyanostilbene-2,2′-disulfonic acid binding. *J. Gen. Physiol. 101*, 715−732.

(22) Jungnickel, B., and Rapoport, T. A. (1993) DIDS (4,4′-diisothiocyanatostilbene-2,2′-disulfonic acid) inhibits an early step of protein translocation across the mammalian ER membrane. *FEBS Lett. 329*, 268−272.

(23) Feng, B. Y., and Shoichet, B. K. (2006) A detergent-based assay for the detection of promiscuous inhibitors. *Nat. Protoc. 1*, 550−553.

(24) Forneris, F., Orru, R., Bonivento, D., Chiarelli, L. R., and Mattevi, A. (2009) ThermoFAD, a Thermofluor®-adapted flavin ad hoc detection system for protein folding and ligand binding. *FEBS J. 276*, 2833−2840.

(25) Salminen, A., Lehtonen, M., Paimela, T., and Kaarniranta, K. (2010) Celastrol: Molecular targets of Thunder God Vine. *Biochem. Biophys. Res. Commun. 394*, 439−442.

(26) Sreeramulu, S., Gande, S. L., Göbel, M., and Schwalbe, H. (2009) Molecular Mechanism of Inhibition of the Human Protein Complex Hsp90−Cdc37, a Kinome Chaperone−Cochaperone, by Triterpene Celastrol. *Angew. Chem., Int. Ed. 48*, 5853−5855.

(27) Klaic, L., Trippier, P. C., Mishra, R. K., Morimoto, R. I., and Silverman, R. B. (2011) Remarkable stereospecific conjugate additions to the Hsp90 inhibitor celastrol. *J. Am. Chem. Soc. 133*, 19634−19637.

DOI: 10.1021/acschembio.6b00666
ACS Chem. Biol. 2016, 11, 3035−3042

(28) Schwyn, B., and Neilands, J. B. (1987) Universal chemical assay for the detection and determination of siderophores. *Anal. Biochem. 160*, 47−56.
(29) Hersman, L., Huang, A., Maurice, P., and Forsythe, J. (2000) Siderophore Production and Iron Reduction by Pseudomonas mendocina in Response to Iron Deprivation. *Geomicrobiol. J. 17*, 261−273.
(30) Leal, S. M., Jr., Roy, S., Vareechon, C., Carrion, S. d., Clark, H., Lopez-Berges, M. S., diPietro, A., Schrettl, M., Beckmann, N., Redl, B., Haas, H., and Pearlman, E. (2013) Targeting Iron Acquisition Blocks Infection with the Fungal Pathogens Aspergillus fumigatus and *Fusarium oxysporum*. *PLoS Pathog. 9*, e1003436.
(31) Meyer, J. M., Neely, A., Stintzi, A., Georges, C., and Holder, I. A. (1996) Pyoverdin is essential for virulence of Pseudomonas aeruginosa. *Infect. Immun. 64*, 518−523.
(32) Lamb, A. L. (2015) Breaking a pathogen's iron will: Inhibiting siderophore production as an antimicrobial strategy. *Biochim. Biophys. Acta, Proteins Proteomics 1854*, 1054−1070.
(33) Tripathi, A., Schofield, M. M., Chlipala, G. E., Schultz, P. J., Yim, I., Newmister, S. A., Nusca, T. D., Scaglione, J. B., Hanna, P. C., Tamayo-Castillo, G., and Sherman, D. H. (2014) Baulamycins A and B, Broad-Spectrum Antibiotics Identified as Inhibitors of Siderophore Biosynthesis in Staphylococcus aureus and Bacillus anthracis. *J. Am. Chem. Soc. 136*, 1579−1586.
(34) Meneely, K. M., Luo, Q., Riley, A. P., Taylor, B., Roy, A., Stein, R. L., Prisinzano, T. E., and Lamb, A. L. (2014) Expanding the results of a high throughput screen against an isochorismate-pyruvate lyase to enzymes of a similar scaffold or mechanism. *Bioorg. Med. Chem. 22*, 5961−5969.
(35) Ferreras, J. A., Ryu, J.-S., Di Lello, F., Tan, D. S., and Quadri, L. E. N. (2005) Small-molecule inhibition of siderophore biosynthesis in Mycobacterium tuberculosis and Yersinia pestis. *Nat. Chem. Biol. 1*, 29−32.
(36) Pinto, L. J., and Moore, M. M. (2009) Screening method to identify inhibitors of siderophore biosynthesis in the opportunistic fungal pathogen, Aspergillus fumigatus. *Lett. Appl. Microbiol. 49*, 8−13.
(37) Hu, Y., Qi, Y., Liu, H., Fan, G., and Chai, Y. (2013) Effects of celastrol on human cervical cancer cells as revealed by ion-trap gas chromatography-mass spectrometry based metabolic profiling. *Biochim. Biophys. Acta, Gen. Subj. 1830*, 2779−2789.
(38) Allison, A. C., Cacabelos, R., Lombardi, V. R. M., Álvarez, X. A., and Vigo, C. (2001) Celastrol, a potent antioxidant and anti-inflammatory drug, as a possible treatment for Alzheimer's disease. *Prog. Neuro-Psychopharmacol. Biol. Psychiatry 25*, 1341−1357.
(39) Kim, D. H., Shin, E. K., Kim, Y. H., Lee, B. W., Jun, J. G., Park, J. H. Y., and Kim, J. K. (2009) Suppression of inflammatory responses by celastrol, a quinone methide triterpenoid isolated from Celastrus regelii. *Eur. J. Clin. Invest. 39*, 819−827.
(40) Nanjundaiah, S. M., Venkatesha, S. H., Yu, H., Tong, L., Stains, J. P., and Moudgil, K. D. (2012) Celastrus and Its Bioactive Celastrol Protect against Bone Damage in Autoimmune Arthritis by Modulating Osteoimmune Cross-talk. *J. Biol. Chem. 287*, 22216−22226.
(41) Yang, H., Chen, D., Cui, Q. C., Yuan, X., and Dou, Q. P. (2006) Celastrol, a Triterpene Extracted from the Chinese "Thunder of God Vine" Is a Potent Proteasome Inhibitor and Suppresses Human Prostate Cancer Growth in Nude Mice. *Cancer Res. 66*, 4758−4765.
(42) Liu, J., Lee, J., Salazar Hernandez, M.-A., Mazitschek, R., and Ozcan, U. (2015) Treatment of Obesity with Celastrol. *Cell 161*, 999−1011.
(43) Wang, S., Liu, K., Wang, X., He, Q., and Chen, X. (2011) Toxic effects of celastrol on embryonic development of zebrafish (Danio rerio). *Drug Chem. Toxicol. 34*, 61−65.
(44) Kiaei, M., Kipiani, K., Petri, S., Chen, J., Calingasan, N. Y., and Beal, M. F. (2005) Celastrol Blocks Neuronal Cell Death and Extends Life in Transgenic Mouse Model of Amyotrophic Lateral Sclerosis. *Neurodegener. Dis. 2*, 246−254.
(45) Jaquet, V., Marcoux, J., Forest, E., Leidal, K. G., McCormick, S., Westermaier, Y., Perozzo, R., Plastre, O., Fioraso-Cartier, L., Diebold, B., Scapozza, L., Nauseef, W. M., Fieschi, F., Krause, K.-H., and Bedard, K. (2011) NADPH oxidase (NOX) isoforms are inhibited by celastrol with a dual mode of action. *Br. J. Pharmacol. 164*, 507−520.
(46) Tallorin, L., Durrant, J. D., Nguyen, Q. G., McCammon, J. A., and Burkart, M. D. (2014) Celastrol inhibits Plasmodium falciparum enoyl-acyl carrier protein reductase. *Bioorg. Med. Chem. 22*, 6053−6061.
(47) Blat, Y. (2010) Non-Competitive Inhibition by Active Site Binders. *Chem. Biol. Drug Des. 75*, 535−540.
(48) Luo, D.-Q., Wang, H., Tian, X., Shao, H.-J., and Liu, J.-K. (2005) Antifungal properties of pristimerin and celastrol isolated from Celastrus hypoleucus. *Pest Manage. Sci. 61*, 85−90.
(49) Fox, B. G., and Blommel, P. G. (2001) Autoinduction of Protein Expression, In *Curr. Protoc. Protein Sci.*; John Wiley & Sons, Inc., New York.
(50) Csáky, T. Z., Hassel, O., Rosenberg, T., Lång (Loukamo), S., Turunen, E., and Tuhkanen, A. (1948) On the Estimation of Bound Hydroxylamine in Biological Materials. *Acta Chem. Scand. 2*, 450−454.
(51) Robinson, R., and Sobrado, P. (2011) Substrate Binding Modulates the Activity of Mycobacterium smegmatis G, a Flavin-Dependent Monooxygenase Involved in the Biosynthesis of Hydroxamate-Containing Siderophores. *Biochemistry 50*, 8489−8496.
(52) Neumann, C. S., Jiang, W., Heemstra, J. R., Gontang, E. A., Kolter, R., and Walsh, C. T. (2012) Biosynthesis of Piperazic Acid via N5-Hydroxy-Ornithine in Kutzneria spp. 744. *ChemBioChem 13*, 972−976.
(53) Binda, C., Robinson, R. M., Martin del Campo, J. S., Keul, N. D., Rodriguez, P. J., Robinson, H. H., Mattevi, A., and Sobrado, P. (2015) An unprecedented NADPH domain conformation in lysine monooxygenase NbtG provides insights into uncoupling of oxygen consumption from substrate hydroxylation. *J. Biol. Chem. 290*, 12676−12688.
(54) Jiang, Z.-Y., Woollard, A. C. S., and Wolff, S. P. (1990) Hydrogen peroxide production during experimental protein glycation. *FEBS Lett. 268*, 69−71.
(55) Trott, O., and Olson, A. J. (2010) AutoDock Vina: improving the speed and accuracy of docking with a new scoring function, efficient optimization and multithreading. *J. Comput. Chem. 31*, 455−461.
(56) Lang, P. T., Brozell, S. R., Mukherjee, S., Pettersen, E. F., Meng, E. C., Thomas, V., Rizzo, R. C., Case, D. A., James, T. L., and Kuntz, I. D. (2009) DOCK 6: Combining techniques to model RNA-small molecule complexes. *RNA 15*, 1219−1230.
(57) Konetschny-Rapp, S., Huschka, H.-G., Winkelmanne, G. n., and Jung, G. n. (1988) High-performance liquid chromatography of siderophores from fungi. *Biol. Met. 1*, 9−17.

DOI: 10.1021/acschembio.6b00666
ACS Chem. Biol. 2016, 11, 3035−3042

SUPPORTING INFORMATION

Inhibition of the flavin-dependent monooxygenase Siderophore A (SidA) blocks siderophore biosynthesis and *Aspergillus fumigatus* growth

Julia S. Martín del Campo[1], Nancy Vogelaar[2], Karishma Tolani[1], Karina Kizjakina[1], Kim Harich[1], and Pablo Sobrado[1,2]
[1] Department of Biochemistry, [2]Virginia Tech Center for Drug Discovery, Virginia Tech, Blacksburg, VA, 24061

Supplemental Table 1. Complete list of hits obtained in the high throughput screening of the library against SidA.

Supplemental Table 2. Melting temperatures of SidA in the presence of different ligands.

Supplemental Table 3. Observed and calculated masses of purified siderophores.

Supplemental Figure 1. Melting curves of SidA in the presence of L-Orn, $NADP^+$ and celastrol.

Supplemental Figure 2. Picture of the AMM-Fe agar plate with different concentrations of celastrol used to determine MIC.

Supplemental Figure 3. HPLC separation of siderophore extracts.

Supplemental Figure 4. Effect of addition of the celastrol in the production of siderophores in developed fungal cultures.

Tables

Table S1. Resulting hits from HTS against SidA using the probe ADP-TAMRA. Reported anisotropy corresponds to percent of normalized values.

Name	Anisotropy	Name	Anisotropy
Celastrol	60	Baicalin	60
Dihydrocelastrol	62	Clofazimine	27
4,4'-Diisothiocyanostilbene-2,2'-sufonic acid sodium salt	64	Nadide	50
Obtusaquinone	57	Daunorubicin	58
Hematein	57	Flurandrenolide	57
Plumbagin	49	Methylprednisolone	42
Gossypetin	33	Laccaic acid A	17
Pyrogallin	48	Haematoporphyrin	56
Tannic acid	57	Calcein	44
Theaflavin	48	Mesalamine	56
Theaflavin monogallates	40	Meclofenamate sodium	55
Irigenol	48	Fast green FCF	20
Aurin tricarboxylic acid	57	Adenosine phosphate	63
7-Deshydroxypyrogallin-4-carboxylic acid	50	Quinalizarin	60
Brazilin	33	Chicago sky blue	64
Tanshinone IIA sulfonate sodium	59	Koparin	65

Table S2. Melting temperatures of SidA in the presence of different ligands and 2 % DMSO. Values obtained using ThermoFAD method. Samples were done in triplicate.

Ligand	T_m / °C
Reference (no ligand)	47.9 ± 0.8
100 mM L-Orn	48.29 ± 0.03
12.5 mM $NADP^+$	46.68 ± 0.04
Celastrol 20 µM	48.1 ± 0.1
Celastrol 110 µM	47.6 ± 0.2

Table S3. Calculated (Calc.) and observed (Obs.) mass data of ferrated siderophores extracted from *A. fumigatus* cultures and used as rescue compounds**.**

Ionic Form	Fe(III)-TAFC		Fe(III)-FC		Fe(III)FsC	
	Calc.	Obs.	Calc.	Obs.	Calc.	Obs.
H^+	906.7	906.2	770.5	771.2	779.6	779.2
Na^+	928.7	928.3	793.5	793.3	802.5	-

Figures

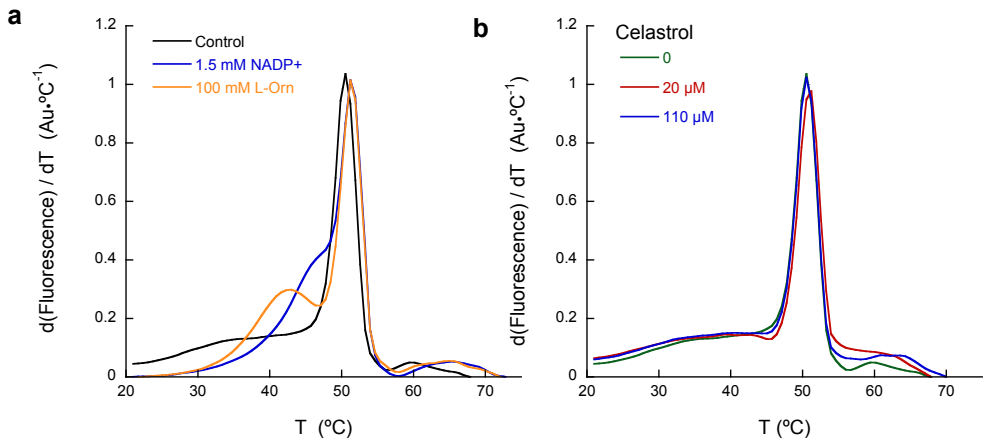

Figure S1. Melting curve of SidA obtained using FAD as the fluorescence probe (ThermoFAD method (1)). Total protein concentration was 3 mg/mL and the final DMSO concentration was 2%. (a) Saturating concentration of $NADP^+$ and L-Orn did not induced changes in the melting temperature. (b) Melting curve of SidA with different celastrol concentration, celastrol does not reduce the melting temperature.

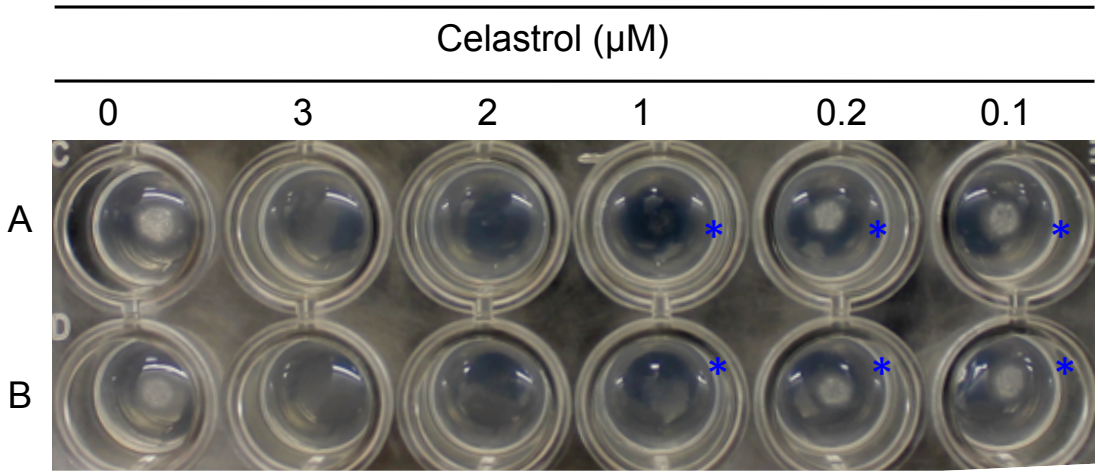

Figure S2. Determination of the minimum inhibitory concentration (MIC) of Celastrol in AMM-Fe after 24 h of incubation at 37 °C. A and B are duplicate samples. The blue mark (*) indicates the presence of growth. At a celastrol concentration of 2 μM no visible growth was observed and this concentration was determined to be the MIC.

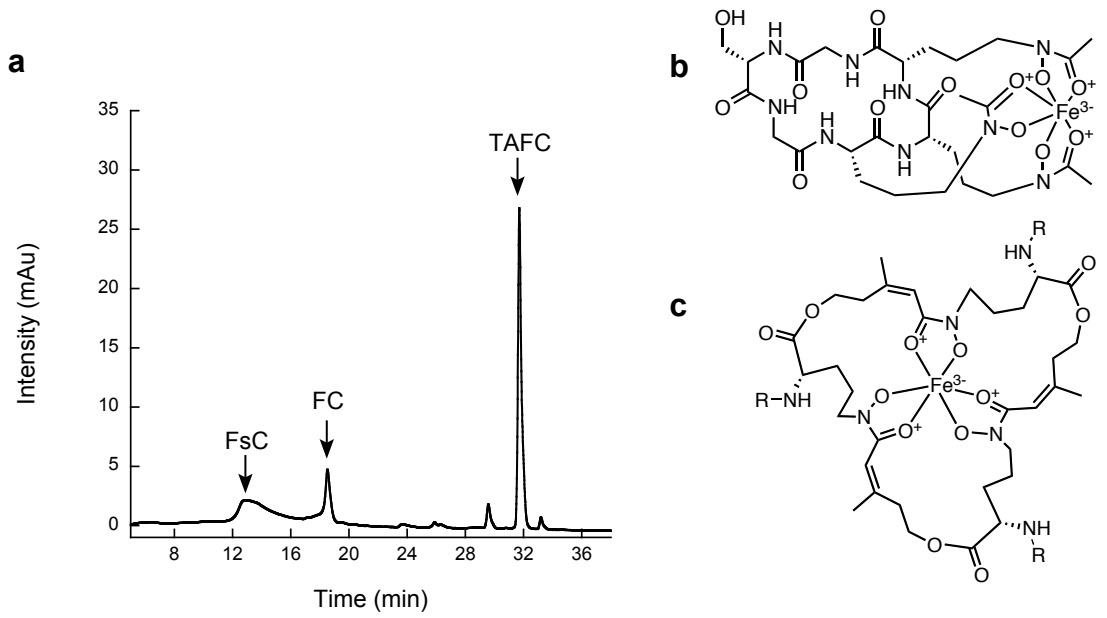

Figure S3. (a) HPLC traces at 435 nm of Fe-siderophores extracted from *Aspergillus fumigatus* cultures. Ferric form of the identified siderophores, (b) Ferricrocin, (c) fusarinine C (FsC) R=H; in triacetylfusarinine C (TAFC) R=acetyl.

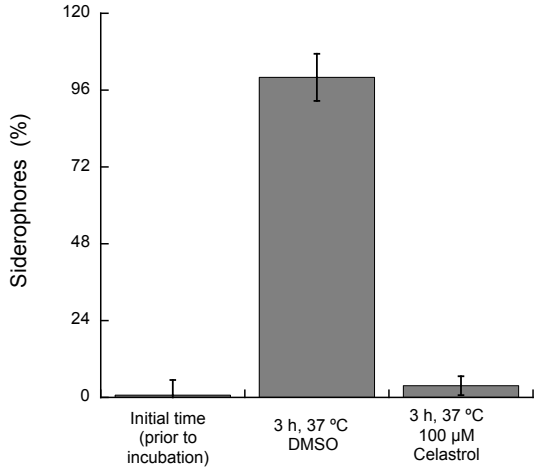

Figure S4. Quantification of extracellular production of siderophores from *A. fumigatus* cultures (grown for 30 h at 37 ºC) produced during three hours incubation (37 ºC) in the presence and absence of 100 µM celastrol. 200 µL agar drops of AMM-Fe were spot-innoculated with $7x10^6$ spores and incubated at 37 °C for 30 h. Agar drops with grown cells were transferred to 2 mL fresh AMM-Fe and incubated for 10 min with continuous stirring. After this time, siderophores in wash solution were quantified with the Chrome Azurol S assay (CAS). A total of three washes were required to remove the siderophores in the agar drop. The first column labeled as initial time corresponds to the residual siderophores in the agar prior to the addition of celastrol (100 µM, 0.5 % DSMO) or DMSO (0.5%). After the third wash the agar drop was transferred into fresh AMM-Fe containing 100 µM celastrol or DSMO and incubated at 37 ºC for 3 h. After this time, siderophores in the liquid phase were quantified using the CAS assay. Siderophore concentration was normalized to the DMSO control. Each sample was done in duplicate.

References

1. Forneris, F., Orru, R., Bonivento, D., Chiarelli, L. R., and Mattevi, A. (2009) ThermoFAD, a Thermofluor®-adapted flavin ad hoc detection system for protein folding and ligand binding. *FEBS J.* **276**, 2833-2840
2. Schwyn, B., and Neilands, J. B. (1987) Universal chemical assay for the detection and determination of siderophores. *Anal. Biochem.* **160**, 47-56